JACS
JOURNAL OF THE AMERICAN CHEMICAL SOCIETY
Article
pubs.acs.org/JACS

H_2-Initiated Reversible Switching between Two-Dimensional Metallacycles and Three-Dimensional Cylinders

Ying-Feng Han,* Long Zhang, Lin-Hong Weng, and Guo-Xin Jin*

Shanghai Key Laboratory of Molecular Catalysis and Innovative Materials, Department of Chemistry, Fudan University, 220 Handan Road, 200433 Shanghai, People's Republic of China

Supporting Information

ABSTRACT: Although reversible covalent activation of molecular hydrogen (H_2) by transition-metal complexes is a common reaction, H_2-mediated sophisticated reversible arrangements of organometallic frameworks have not yet been described. Herein, we report unusual organometallic transformations in solution that can be accomplished by uptake or release of H_2. An efficient route for synthesizing air- and moisture-stable 16-electron M_2L_2-type metallacycles under very mild conditions has been developed. The new organometallic metallacycles favor the binding of small ligands such as MeCN, Cl^-, CO, and pyridine. The reaction of a coordinatively unsaturated 16-electron M_2L_2-type macrocyclic complex featuring thione ligands with 1 atm of H_2 leads to the isolation of a 18-electron M_2L_3-type cylinder, along with hydride species. Remarkably, the obtained mixture underwent loss of H_2 in a facile manner upon heating to re-form the starting M_2L_2-type complex. A possible mechanism is proposed for the reversible transformations.

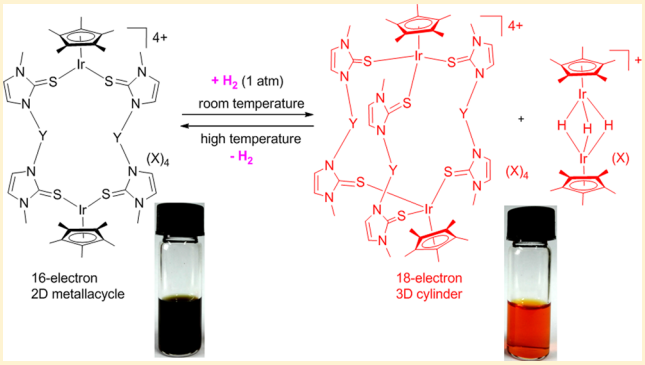

INTRODUCTION

In modern organometallic chemistry, molecular dihydrogen (H_2) is viewed as a fundamental reagent due to its use in most homogeneous catalytic hydrogenations.[1,2] Heterolytic cleavage of the H−H bond is a key step in the function of hydrogenases.[3,4] Various transition-metal complexes[1,2] and main-group elements,[5−7] together with metallic cluster complexes,[8−11] have been used to promote heterolysis of H_2. H_2 also serves as an important ligand in coordination and organometallic chemistry, a fact that has been well demonstrated.[12] Reversible H_2 addition across an M−B bond was recently reported.[13] In the reported examples of transition-metal-catalyzed H_2 activation, it is clear that coordinatively unsaturated organometallic species play a critical role in stoichiometric and catalytic transformations mediated by transition-metal complexes, as either catalyst precursors or key intermediates or both.[14] As a consequence, the isolation and characterization of coordinatively unsaturated organometallic complexes have become some of the most active and exciting areas of current research.[15] However, studies are generally difficult because of the high reactivity of these species, in conjunction with their air and moisture sensitivity.

We entered this arena by targeting air- and moisture-stable, coordinatively unsaturated, organometallic complexes featuring metal−sulfur bonds.[16] We had hoped that using these species in the heterolysis of H_2 mediated by M−S bonds would provide a novel model of [NiFe] hydrogenases.[3,4] An unstable, coordinatively unsaturated iridium complex, bearing a bulky 2,6-dimesitylbenzenethiolate (SDmp) ligand, has been reported by Tatsumi et al.[17] to exhibit activity in the reversible splitting of H_2. Although half-sandwich iridium-/rhodium-catalyzed H_2 activation is well-known,[18] an example of H_2-catalyzed reversible C−H and N−H bond formation in homogeneous organometallic iridium systems was reported only recently.[19] However, even under an H_2 atmosphere (1 atm, room temperature), a complete conversion to the known dinuclear trihydride complex $[Cp^*_2Ir_2(\mu\text{-}H)_3]^+$ occurred, along with the release of free and protonated organic ligands.[20] A similar phenomenon was also observed in the reaction of an unsaturated iridium amide with H_2.[21]

The reversible arrangement of molecular building blocks in self-assembled architectures has led to numerous new and fascinating molecular switching systems and dynamic materials.[22,23] An understanding of the supramolecular chemical evolution of matter in response to different stimuli can provide much information about molecular recognition processes and also offer some opportunities in the design and synthesis of dynamic materials and biologically active molecules.[22−24] Various stimuli such as pH, light, redox processes, and coordination metal ions have been used to compare their effect on self-assembled structures.[25] However, well-controlled structural transformations of discrete self-assembled supramolecules have rarely been studied.[26] A few examples of the

Received: August 20, 2014
Published: September 12, 2014

 © 2014 American Chemical Society

transformation between 2D and 3D discrete structures were described by Stang[27] and Schmittel.[28] A useful supramolecular reaction known as the halide-induced ligand rearrangement reaction has been developed and studied extensively by Mirkin and co-workers.[29] The relative arrangement in heteroligated supramolecular coordination complexes can be regulated in situ using small ancillary ligands such as halides, CO, and nitriles. On the basis of the addition or removal of chemical stimuli, supramolecular allosteric enzyme mimics were designed.[30] Therefore, the design and construction of supramolecular structures through structural transformations triggered by external stimuli is still in demand. In particular, the sophisticated rearrangement between organometallic assemblies, mediated by small organic molecules, is scarce. Some small organic molecules such as N-heterocyclic carbenes have been found to initiate unusual organometallic transformations in solution at room temperature.[31,32]

For these reasons, it was of interest to target new coordinatively unsaturated organometallic complexes based on Cp*M−S fragments in order to investigate potentially new reaction routes for new organometallic assemblies derived therefrom. As described below, this work began with attempts to synthesize a series of coordinatively unsaturated 16-electron organometallic metallacycles as starting materials. An efficient route for synthesizing air- and moisture-stable 16-electron M_2L_2-type metallacycles under very mild conditions has been developed. The new organometallic metallacycles favor the binding of small ligands such as MeCN, Cl^-, CO, and pyridine. Preliminary studies show that some of these new complexes are reactive with H_2. In this context, unusual organometallic switching between 2D 16-electron M_2L_2-type metallacycles and 3D 18-electron M_2L_3-type cylinders in solution was accomplished by uptake or release of H_2.

■ RESULTS AND DISCUSSION

Synthesis of Coordinatively Unsaturated 16-Electron Organometallic Metallacycles. The 16-electron complexes **1a**$(X)_4$ (X^- = OTf^-, NO_3^-, BF_4^-), **1b**$(OTf)_4$, and **2**$(OTf)_4$−**7**$(OTf)_4$, generally formulated as $[(Cp^*M)_2(\mu\text{-}\mathbf{L})_2](X)_4$, were prepared in good yields from the sequential reactions of $[Cp^*MCl_2]_2$ (M = Ir, Rh) with silver salts and the corresponding bidentate organosulfur ligands **L1**−**L7**, as shown in Scheme 1 and Table 1. The structures of coordinatively unsaturated 16-electron macrocyclic complexes were unambiguously confirmed by single-crystal X-ray diffraction studies of **1a**$(X)_4$ (X^- = OTf^-, NO_3^-, BF_4^-), **1b**$(OTf)_4$, **3**$(OTf)_4$, **5**$(OTf)_4$, **6**$(OTf)_4$, and **7**$(OTf)_4$. The examples of **1a**$(OTf)_4$, **3**$(OTf)_4$, **5**$(OTf)_4$, **6**$(OTf)_4$, and **7**$(OTf)_4$ are shown in Figure 1. Selected bond lengths and angles are summarized in Table S1 in the Supporting Information.

Scheme 1. Synthesis of Coordinatively Unsaturated 16-Electron Organometallic Metallacycles

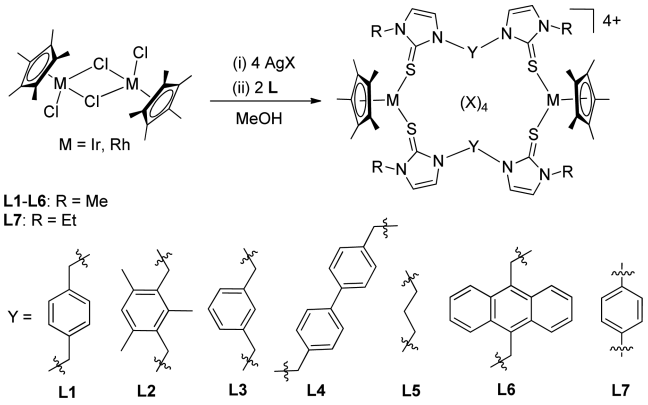

Table 1. Scope of Formation of 16-Electron Organometallic Metallacycles[a]

entry	M	AgX	L	product	yield (%)[b]
1	Ir	AgOTf	**L1**	**1a**$(OTf)_4$	88
2	Ir	$AgNO_3$	**L1**	**1a**$(NO_3)_4$	89
3	Ir	$AgBF_4$	**L1**	**1a**$(BF_4)_4$	91
4	Rh	AgOTf	**L1**	**1b**$(OTf)_4$	82
5	Ir	AgOTf	**L2**	**2**$(OTf)_4$	88
6	Ir	AgOTf	**L3**	**3**$(OTf)_4$	90
7	Ir	AgOTf	**L4**	**4**$(OTf)_4$	90
8	Ir	AgOTf	**L5**	**5**$(OTf)_4$	87
9	Ir	AgOTf	**L6**	**6**$(OTf)_4$	87
10	Ir	AgOTf	**L7**	**7**$(OTf)_4$	81

[a]Reaction conditions: AgOTf (0.2 mmol), $[Cp^*MCl_2]_2$ (0.05 mmol), and **L** (0.1 mmol) in MeOH (20 mL). [b]Isolated product yields are given.

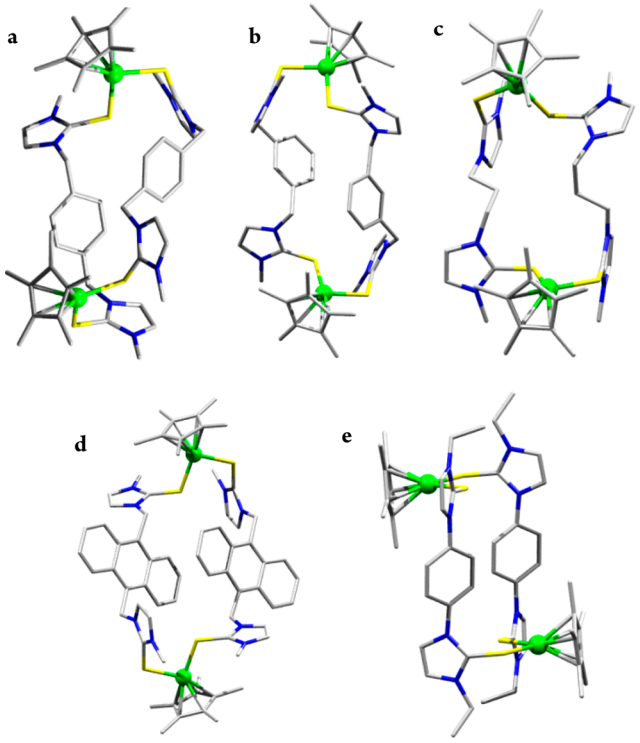

Figure 1. Wire frame representations (with metal atoms shown as space-filling spheres) of the single-crystal X-ray structures of the cationic parts of molecular rectangles: (a) **1a**$(OTf)_4$, (b) **3**$(OTf)_4$, (c) **5**$(OTf)_4$, (d) **6**$(OTf)_4$, (e) **7**$(OTf)_4$. Color code: Ir, green; S, yellow; N, blue; C, gray.

As shown in Figure 1, each of the molecules has a dimeric stucture that is composed of two $[Cp^*M(\mu\text{-}\mathbf{L})]$ units with the metal atoms being surrounded by two S atoms from different ligands. It is worth noting that the structures are coordinatively unsaturated 16-electron two-dimensional metallacycles. No coordinating solvent was observed in the structures. All

complexes are air and moisture stable. The solubility of these complexes is not good in normal solvents such as $CHCl_3$, CH_2Cl_2, THF, and toluene, but the complexes are soluble in MeOH.

The coordination geometry around the metal center is almost a two-legged piano stool, and the S−M−S bond angle is aproximately 90°. The average Ir−S bond length (ca. 2.30 Å) in iridium complexes is shorter than that of the reported 18-electron half-sandwich complex Cp*Ir(PMe_3)Cl(SDmp) (2.42 Å); however, it is slightly longer than that of the cationic 16-electron half-sandwich complex [Cp*Ir(PMe_3)(SDmp)]$^+$ (2.21 Å).[17] Similarly, the average Rh−S bond length (2.32 Å) in the rhodium complex **1b**(OTf)$_4$ is shorter than that of saturated thiolate complexes of rhodium but still longer than those of unsaturated Cp*Rh(PMe_3)(SDmp)$^+$ (2.21 Å).[17]

H_2-Initiated Transformation Reactions. Preliminary studies show that the complex **1a**(OTf)$_4$ is reactive toward H_2. Exposure of a dark green CD_3OD solution of **1a**(OTf)$_4$ to 1 atm of H_2 at room temperature resulted in a red solution. To our surprise, the complex [(Cp*Ir)$_2$(μ-**L1**)$_3$](OTf)$_4$ (**8**(OTf)$_4$) was isolated in 89% yield (based on **L1**) as red crystals (Scheme 2). The reaction was monitored by its ^{1}H NMR spectrum in

Scheme 2. H_2-Mediated Transformation Reactions from 16-Electron to 18-Electron Species

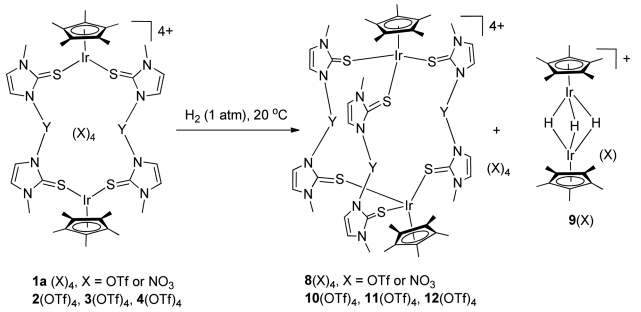

CD_3OD, showing that **8**(OTf)$_4$ was formed quantitatively together with the dinuclear trihydride [Cp*$_2$Ir$_2$(μ-H)$_3$](OTf) (**9**(OTf)).[33] The dinuclear trihydride complex **9**(OTf) can be easily isolated. Subsequent ^{1}H NMR analysis and a single-crystal X-ray diffraction study confirmed the formulation of this species (Figure S1, Supporting Information).[34] Similarly, under an atmosphere of H_2, a CD_3OD solution of the complex **1a**(NO_3)$_4$ was completely converted into complex **8**(NO_3)$_4$ along with **9**(NO_3), over the course of 2 h. Whereas in complex **1a**(NO_3)$_4$ the methylene group of the ligand and methyl group from the Cp* ring appear in the ^{1}H NMR spectrum as signals at δ 5.15 (broad) and 1.70 ppm in a 4:15 ratio of relative intensity, in complex **8**(NO_3)$_4$, these two signals are replaced by two resonances at 5.83 (broad) and 1.51 ppm in a 6:15 ratio of relative intensity (Figure 2). The last two signal ratios indicate that the **L1**:Cp*Ir ratio should be 3:2. The resonance attributed to the Cp* ring shifted from 1.70 to 1.51 ppm, consistent with a change in valence electron count of the metal center from 16 electrons to 18 electrons. The broad singlet corresponding to the methylene group in the ^{1}H NMR spectra indicates the rapid rotation of bridging ligands in CD_3OD solution at room temperature.

The directing role of the H_2-initiated transformation reaction was further investigated by expanding the choice of thionated ligands. Surprisingly, we have found that the internal bridged pattern can influence the reactivity of the reactions. Under

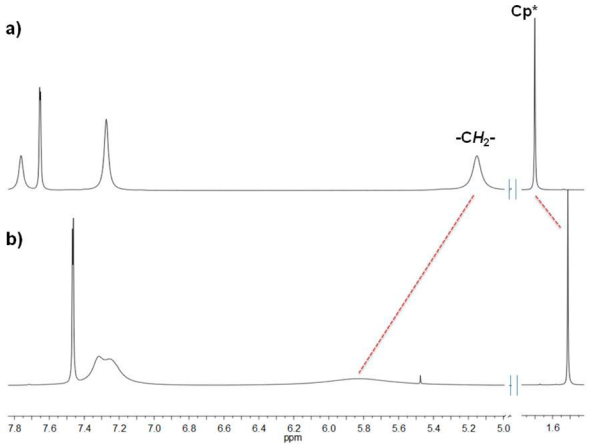

Figure 2. Partial ^{1}H NMR spectra (400 MHz, 300 K) of (a) **1a**(NO_3)$_4$ and (b) **8**(NO_3)$_4$ in CD_3OD.

similar reaction conditions, it was observed that the reactivity of transformations with **2**(OTf)$_4$−**4**(OTf)$_4$ is similar to that with **1**(OTf)$_4$. In all cases, the corresponding pure 18-electron complexes **10**(OTf)$_4$−**12**(OTf)$_4$ were obtained in high yields. The formation of complexes **10**(OTf)$_4$ and **12**(OTf)$_4$, cylindrical M_2L_3 species, were determined by single-crystal X-ray crystallographic analyses. In contrast, the reactions of **6**(OTf)$_4$ and **7**(OTf)$_4$ with H_2 are very difficult. In the case of **6**(OTf)$_4$, the formation of a type of M_2L_3 complex is difficult due to the crowding of the anthracene ligand. In the case of **7**(OTf)$_4$, presumably the rigidity of the ligand inhibits the formation of the M_2L_3 complex. This information indicates that the selection of the right flexible bridging ligand is important. In our system, the flexibility of ligands **L1**−**L4**, in which two thione units are connected to a central aromatic core via methylene groups, allows the assembly of ligands to adopt whatever conformations are needed to satisfy the coordination requirements of metal centers by the free rotation of the thione ring around the methylene spacers.[35] In addition, the size of the bridging ligands should also be considered. It is worth noting that the reaction with H_2 is solvent dependent, as discussed below.

Most interestingly, we have found that the obtained mixture containing an M_2L_3-type 18-electron complex and the iridium hydride species underwent loss of H_2 in a facile manner. For example, when argon was purged through a red solution obtained from the reaction of complex **1a**(OTf)$_4$ and H_2 in MeOH solution at 80 °C for 5 h, the color changed to dark green; complex **1a**(OTf)$_4$ was formed and isolated in a yield of 67%. Again, when the obtained solution containing complexes **10**(OTf)$_4$ and **9**(OTf) from the reaction of complexes **2**(OTf)$_4$ and H_2 was heated at 80 °C under an argon stream, complex **2**(OTf)$_4$ and H_2 were regenerated, and complex **2**(OTf)$_4$ was isolated in 68% yield as crystals. UV titration experiments also supported this reversible conversion (Figure 3). In both cases, when the obtained mixture in CD_3OD was heated to 80 °C for 1 h in a sealed NMR tube, the formation of hydrogen was confirmed by the observation of a signal at 4.58 ppm by ^{1}H NMR spectroscopy.

Structures of 18-Electron Organometallic Cylinders. The single-crystal X-ray structures of **8**(OTf)$_4$, **8**(NO_3)$_4$, **10**(OTf)$_4$, and **12**(OTf)$_4$ were determined. The crystal structures revealed the cation of each complex to be a five-component, three-dimensional binuclear metallosupramolecu-

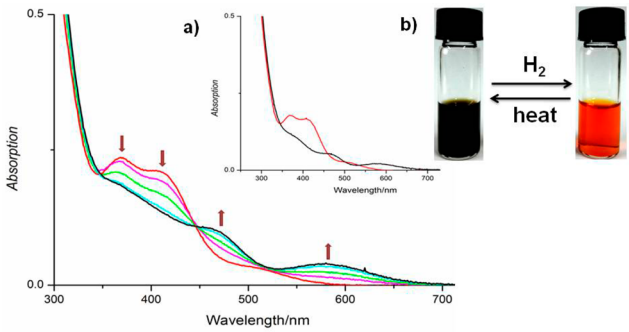

Figure 3. UV−visible titration of the regeneration of $2(OTf)_4$ from a mixture in MeOH at high temperature (the mixture was obtained from reaction of $2(OTf)_4$ and H_2). Inserts: (a) UV−visible spectra of complexes $2(OTf)_4$ (black line) and $10(OTf)_4$ (red line) in CH_3OH; (b) interconversion of methanol solutions of 16-electron (dark) and 18-electron (red) species.

lar cylinder, as shown in Figure 4. Selected bond lengths and angles of them are summarized in Table S2 (Supporting Information). Two Cp*Ir units are bridged by three corresponding thione ligands. In each complex, the iridium atom adopts a typical three-legged piano-stool conformation and was coordinated by three sulfur atoms and a Cp* ring. The average Ir−S bond length (ca. 2.43 Å) in all complexes is notably longer than those of coordinatively unsaturated 16-electron organometallic metallacycles (ca. 2.30 Å), owing to the 18-valence-electron count of the metal center. However, the bond length is still consistent with those of the reported 18-electron half-sandwich complexes.[17]

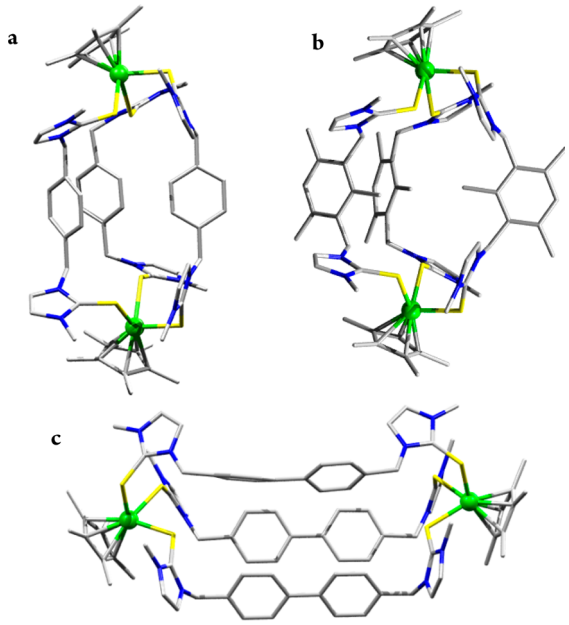

Figure 4. Wire frame representations (with metal atoms shown as space-filling spheres) of the single-crystal X-ray structures of the cationic parts of molecular cylinders: (a) $8(OTf)_4$; (b) $10(OTf)_4$; (c) $12(OTf)_4$. Color code: Ir, green; S, yellow; N, blue; C, gray.

Reactions of 16-Electron Metallacycles. As expected for coordinatively unsaturated 16-electron iridium species, complexes $1a(OTf)_4$ and $2(OTf)_4$ bind a wide range of ligands (Scheme 3). The dissolution of $2(OTf)_4$ in CD_3CN led instantly to a light yellow solution, giving the expected CD_3CN adduct $2(NCMe)_2](OTf)_4$. The MeCN ligands are labile and can be removed by subjecting the solution to a vacuum, as signaled by a color change from yellow to dark green.

Scheme 3. Reactivity of 16-Electron Metallacycles

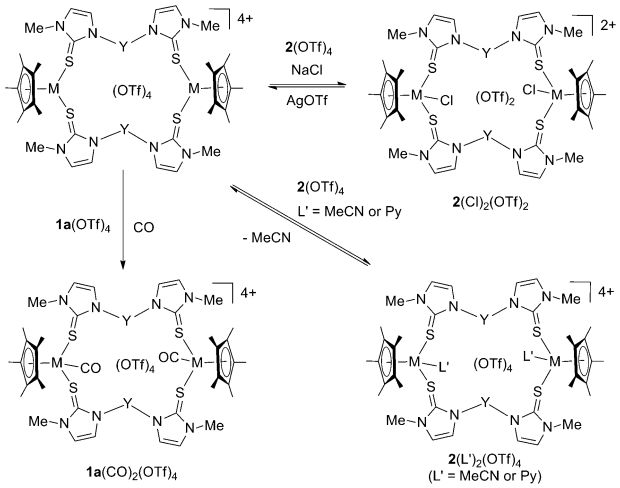

Addition of CO to a dark green solution of $1a(OTf)_4$ in MeOH resulted in formation of a light yellow solution of $[1a(CO)_2](OTf)_4$ in a few minutes. The ^1H NMR (CD_3OD) spectra revealed a significant shift for the protons of the Cp* ring in comparison with those of the 16-electron complex $1a(OTf)_4$. Two carbon signals for coordinated CO were observed in the ^{13}C NMR (CD_3OD) spectrum at ca. 170 ppm. The reaction of pyridine (Py) with $2(OTf)_4$ induced complete conversion to the pyridine adduct $[2(Py)_2](OTf)_4$ quickly, as signaled by a color change from dark blue to yellow. The chloride complex $[2(Cl)_2](OTf)_2$ was prepared from the reaction of NaCl and $2(OTf)_4$. Chloride abstraction of the complex $[2(Cl)_2](OTf)_2$ by AgOTf in a simple manner led to instantaneous formation of the complex $2(OTf)_4$.

The solid-state molecular structures of $[2(Py)_2](OTf)_4$ and $[2(Cl)_2](OTf)_2$ were determined by single-crystal X-ray crystallographic studies (Figure 5a,b). Selected bond lengths and angles are summarized in Table S3 in the Supporting Information. These species were found to be binuclear complexes in which the iridium is coordinated by two sulfur atoms (from different ligands) and one nitrogen atom from the Py of $[2(Py)_2](OTf)_4$ or the chloride atom of $[2(Cl)_2](OTf)_2$.

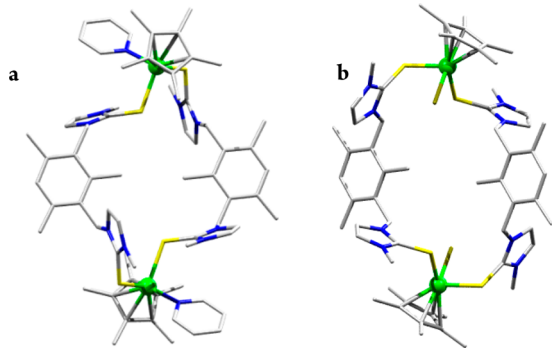

Figure 5. Wire frame representations (with metal atoms shown as space-filling spheres) of the single-crystal X-ray structures of the cationic parts of molecular rectangles: (a) $2(Py)_2(OTf)_4$; (b) $2(Cl)_2(OTf)_2$. Color code: Ir, green; S, yellow; N, blue; C, gray; Cl, dark yellow.

dx.doi.org/10.1021/ja508543y | J. Am. Chem. Soc. 2014, 136, 14608−14615

The Ir−S bond lengths in $[\mathbf{2}(Py)_2](OTf)_4$ and $[\mathbf{2}(Cl)_2](OTf)_2$ (ca. 2.42 Å) are notably longer than those of the 16-electron complexes (ca. 2.30 Å) but are close to those of the 18-electron cylindrical complexes.

Proposed Mechanism. Stirring the MeOH solution of coordinatively unsaturated 16-electron organometallic metallacycles such as $\mathbf{1a}(X)_4$ (X^- = OTf^-, NO_3^-) and $\mathbf{2}(OTf)_4$ in the absence of H_2 at 20 °C for several days did not lead to any reaction, meaning that the organometallic framework transformation is initiated by H_2. In addition, MeCN inhibits the hydrogenolysis by preventing formation of the η^2-H_2 intermediate. It seems probable that H_2 may first coordinate to the coordinatively unsaturated metal center, forming key η^2-H_2 intermediates[19] (structurally analogous to $[\mathbf{1a}(CO)_2](OTf)_4$ or $[\mathbf{2}(Py)_2](OTf)_4$), and then the subsequent splitting of H_2 occurs. When the hydride iridium species is formed, the released free ligand may coordinate to the coordinatively unsaturated metal center, rapidly leading to the 18-electron M_2L_3-type complex as described above. Once formed, the 18-electron M_2L_3-type complex becomes stable toward H_2. When the mixture is heated at high temperature, the hydride iridium species will lose H_2 to give $[Cp^*Ir]^{2+}$ dications,[20] and then the 16-electron complex is regenerated. It seems that a reversible structural changeover between discrete 2D metallacyclic and 3D cylindrical assemblies can be effected simply by tuning the thione ligand/$[Cp^*Ir]^{2+}$ ratio. The selective formation of binuclear double-$[M_2L_2]$ and triple-stranded $[M_2L_3]$ complexes can be controlled, depending on the metal/ligand ratio or topology of the ligands.[28,36]

To confirm this mechanistic hypothesis, further experimental work was performed. The rapidity of reactions of H_2 with 16-electron metallacycles suggests that a low-temperature search for the intermediates might be informative. First, combining complex $\mathbf{1a}(OTf)_4$ with 1 atm of H_2 in CD_3OD at −78 °C and then recording ^{1}H NMR spectra at −40 °C after 10 min showed the formation of a η^2-H_2 adduct (structurally analogous to its carbonyl or pyridine adducts).[19] Upon warming to 0 °C over 20 min, a mixture of starting material $\mathbf{1a}(OTf)_4$, the 18-electron η^2-H_2 adduct, and $\mathbf{8}(OTf)_4$ were observed (Figure 6).

At room temperature (26 °C), the η^2-H_2 adduct disappeared and the rate of the transformation from $\mathbf{1a}(OTf)_4$ to $\mathbf{8}(OTf)_4$ became fast, while the corresponding hydride signals were observed at high field.[20] Second, stirring isolated M_2L_3-type complexes under a H_2 atmosphere for 1 week did not lead to any change. However, upon addition of 0.5 equiv of $[Cp^*Ir]^{2+}$ dications to solutions of $\mathbf{8}(OTf)_4$ and $\mathbf{10}(OTf)_4$ in CD_3OD, conversion to $\mathbf{1a}(OTf)_4$ and $\mathbf{2}(OTf)_4$ occurred rapidly. Third, when **L2** was added to a dark green solution of complex $\mathbf{2}(OTf)_4$ in CD_3OD, a rapid color change to a clear red solution was observed and a new set of signals for complex $\mathbf{10}(OTf)_4$ appeared in the ^{1}H NMR spectrum; the signals of complex $\mathbf{2}(OTf)_4$ completely disappeared when the ligand to metal ratio reached 3:2. On the basis of these results, the transformation between the two organometallic species is presumed to occur via the aforementioned mechanistic route.

■ CONCLUDING REMARKS

In general, we have found that H_2 can initiate unusual transformations between organometallic assemblies. If the Cp* group acts as a monodentate ligand, then the reversible constitutional switching between the two distinct complexes is accompanied by reversible changes in the coordination mode of the metal center from triangular to tetrahedral coordination geometries. The present system reversibly provides a foundation on which to develop organometallic switching systems that can be triggered by hydrogen.

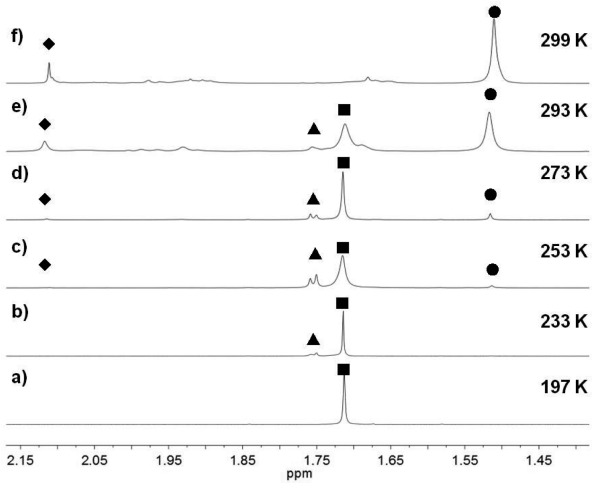

Figure 6. Variable-temperature ^{1}H NMR studies of reaction of complex $\mathbf{1a}(OTf)_4$ and H_2 (only partial region for the proton of Cp* ring was shown) in CD_3OD: (a) 197 K; (b) 233 K, 10 min; (c) 253 K, 20 min; (d) 273 K, 30 min; (e) 293 K, 40 min; (f) 299 K, 70 min. Legend: (●) $\mathbf{1a}(OTf)_4$; (▲) η^2-H_2 adduct; (■) $\mathbf{8}(OTf)_4$; (♦) $\mathbf{9}(OTf)$.

■ EXPERIMENTAL SECTION

General Procedures. All experiments were conducted under nitrogen using standard Schlenk techniques. Nondeuterated solvents were distilled under N_2 from appropriate drying agents. The compounds $[Cp^*IrCl_2]_2$,[37] $[Cp^*RhCl_2]_2$,[37] and thione ligands (for details, see the Supporting Information)[38] were prepared according to literature procedures. All other chemicals were purchased from commercial sources and used without further purification. NMR spectra were recorded on Bruker AVANCE I 400 and VANCE-DMX 500 spectrometers. Spectra were recorded at room temperature unless otherwise noted and referenced to the residual protonated solvent for NMR spectra. Coupling constants are expressed in hertz. Complex multiplets are noted as "m" and broad resonances as "br". Mass spectra were obtained with MicroTof (Bruker Daltonics, Bremen), Quattro LCZ (Waters-Micromass, Manchester, U.K.), and Varian MAT 212 spectrometers. Elemental analyses were performed with an Elementar Vario EL III analyzer. All of the samples were dried under vacuum at 80 °C over 24 h before analysis.

Synthesis of Coordinatively Unsaturated 16-Electron Organometallic Metallacycles. *Preparation of $[Cp^*_2Ir_2(\mu\text{-}\mathbf{L1})_2](OTf)_4$ ($\mathbf{1a}(OTf)_4$).* AgOTf (51 mg, 0.2 mmol) was added to a solution of $[Cp^*IrCl_2]_2$ (40 mg, 0.05 mmol) in CH_3OH (20 mL) at room temperature. The reaction mixture immediately turned pale yellow from orange, and white solid AgCl precipitated from the solution over the course of 10 min. The obtained suspension was filtered. **L1** (33 mg, 0.1 mmol) was added to the filtrate. A rapid color change from pale yellow to dark green was observed. The mixture was stirred at room temperature for 2 h. The solvent was concentrated to 2 mL and diethyl ether added. The resulting dark green solid was collected by filtration and dried under vacuum to give the complex $\mathbf{1a}(OTf)_4$ (84 mg, 88%). ^{1}H NMR (400 MHz, CD_3OD, ppm): δ 1.71 (s, 30H, Cp*), 3.82 (br, 12H, CH_3), 5.25 (br, 8H, $-CH_2-$), 7.23−7.65 (16H, Ar-H and thione). ^{1}H NMR (500 MHz, CD_3OD, ppm, −40 °C): δ 1.71 (s, 30H, Cp*), 3.78 (s, 6H, N-CH_3), 3.84 (s, 6H, N-CH_3), 4.41 (d, J = 13.9 Hz, 2H, $-CH_2-$), 5.22 (d, J = 14.4 Hz, 2H, $-CH_2-$), 5.30 (d, J = 13.8 Hz, 2H, $-CH_2-$), 5.53 (d, J = 14.1 Hz, 2H, $-CH_2-$), 7.00 (d, J = 8.0 Hz, 4H, Ar-H), 7.59−7.62 (m, 6H, thione and Ar-H), 7.63 (d, J = 1.8 Hz, 2H, thione), 7.73 (d, J = 2.1 Hz, 2H, thione), 8.13 (d, J = 2.1 Hz, 2H, thione). $^{13}C\{^1H\}$ NMR (125 MHz, CD_3OD, ppm): δ 9.96

(Cp*-CH_3), 50.00 (N-CH_3), 52.77 (CH_2), 96.63 (Cp*-C), 121.85 (SO_3CF_3, J_{CF} = 319.6 Hz), 123.43, 125.97, 131.36 (br), 136.66, 148.81 (C═S). ^{19}F NMR (376 MHz, CD_3OD, ppm): δ −79.84. Anal. Calcd for $C_{56}H_{66}F_{12}Ir_2N_8O_{12}S_8$: C, 35.18; H, 3.48; N, 5.86. Found: C, 35.17; H, 3.29; N, 5.92. MS (ESI, positive ions): m/z 807.1295 (calcd for [M − 2OTf]$^{2+}$ 807.1296), 1763.2138 (calcd for [M − OTf]$^+$ 1763.2138).

Preparation of [Cp$_2$Ir$_2$(μ-**L1**)$_2$](NO$_3$)$_4$ (**1a**(NO$_3$)$_4$).* This reaction was carried out as for **1a**(OTf)$_4$, using $AgNO_3$ (34 mg, 0.2 mmol), [Cp*$IrCl_2$]$_2$ (40 mg, 0.05 mmol), and **L1** (33 mg, 0.1 mmol) in MeOH solution. **1a**(NO_3)$_4$ was isolated as a dark green solid (70 mg, 89%). ^{1}H NMR (400 MHz, CD_3OD, ppm): δ 1.70 (s, 30H, Cp*), 3.82 (s, 12H, N-CH_3), 5.15 (br s, 8H, −CH_2−), 7.27 (s, 8H, Ar-H), 7.65 (d, J = 1.9 Hz, 4H, thione), 7.76 (br, 4H, thione). ^{13}C{^{1}H} NMR (101 MHz, CD_3OD, ppm): δ 9.80 (Cp*-CH_3), 36.79 (N-CH_3), 52.76 (CH_2), 96.51 (Cp*-C), 123.69, 125.91, 131.31 (br), 136.61, 148.79 (C═S). Anal. Calcd for $C_{52}H_{66}Ir_2N_{12}O_{12}S_4$: C, 39.94; H, 4.25; N, 10.75. Found: C, 39.72; H, 4.21; N, 10.93. MS (ESI, positive ions): m/z 719.9188 (calcd for [M − 2NO_3]$^{2+}$ 719.9189).

[Cp$_2$Ir$_2$(μ-**L1**)$_2$](BF$_4$)$_4$ (**1a**(BF$_4$)$_4$).* This reaction was carried out as for **1a**(OTf)$_4$, using $AgBF_4$ (39 mg, 0.2 mmol), [Cp*$IrCl_2$]$_2$ (40 mg, 0.05 mmol), and **L1** (33 mg, 0.1 mmol) in MeOH solution. **1a**(BF_4)$_4$ was isolated as a dark green solid (76 mg, 91%). ^{1}H NMR (400 MHz, DMSO-d_6, ppm): δ 1.62 (s, 30H, Cp*), 3.81 (s, 12H, N-CH_3), 5.19−5.26 (m, 8H, −CH_2−), 7.08 (s, 8H, Ar-H), 7.47 (br s, 4H, thione), 7.78 (s, 4H, thione).

[Cp$_2$Rh$_2$(μ-**L1**)$_2$](OTf)$_4$ (**1b**(OTf)$_4$).* This reaction was carried out as for **1a**(OTf)$_4$, using AgOTf (51 mg, 0.2 mmol), [Cp*$RhCl_2$]$_2$ (31 mg, 0.05 mmol), and **L1** (33 mg, 0.1 mmol) in MeOH solution. **1b**(OTf)$_4$ was isolated as a dark green solid (71 mg, 82%). ^{1}H NMR (400 MHz, CD_3OD, ppm): δ 1.68 (s, 30H, Cp*), 3.80 (s, 12H, N-CH_3), 5.26 (br, 8H, −CH_2−), 7.28−7.49 (br, 16H, Ar-H and thione). Anal. Calcd for $C_{56}H_{66}F_{12}Rh_2N_8O_{12}S_8$: C, 38.80; H, 3.84; N, 6.46. Found: C, 38.52; H, 3.46; N, 6.18.

[Cp$_2$Ir$_2$(μ-**L2**)$_2$](OTf)$_4$ (**2**(OTf)$_4$).* This reaction was carried out as for **1a**(OTf)$_4$, using AgOTf (51 mg, 0.2 mmol), [Cp*$IrCl_2$]$_2$ (40 mg, 0.05 mmol), and **L2** (37 mg, 0.1 mmol) in MeOH solution. **2**(OTf)$_4$ was isolated as a dark green solid (88 mg, 88%). ^{1}H NMR (400 MHz, CD_3OD, ppm): δ 1.77 (s, 30H, Cp*), 2.31 (br, 18H, CH_3), 3.85, 3.91 (12H, N-CH_3), 5.39 (m, 8H, −CH_2−), 7.01−7.61 (10H, thione and Ar-H). Anal. Calcd for $C_{62}H_{78}F_{12}Ir_2N_8O_{12}S_8$: C, 37.30; H, 3.94; N, 5.61. Found: C, 37.45; H, 3.59; N, 5.22. MS (ESI, positive ions): m/z 516.4665 (calcd for [M − 3OTf]$^{3+}$ 516.4670), 849.1765 (calcd for [M − 2OTf]$^{2+}$ 849.1766), 1847.3078 (calcd for [M − OTf]$^+$ 1847.3052).

[Cp$_2$Ir$_2$(μ-**L3**)$_2$](OTf)$_4$ (**3**(OTf)$_4$).* This reaction was carried out as for **1a**(OTf)$_4$, using AgOTf (51 mg, 0.2 mmol), [Cp*$IrCl_2$]$_2$ (40 mg, 0.05 mmol), and **L3** (33 mg, 0.1 mmol) in MeOH solution. **3**(OTf)$_4$ was isolated as a dark green solid (85 mg, 90%). ^{1}H NMR (400 MHz, CD_3OD, ppm): δ 1.70 (s, 30H, Cp*), 3.82 (s, 12H, N-CH_3), 5.16 (br, 8H, −CH_2−), 6.95 (br, 4H), 7.36 (m, 2H, Ar-H), 7.65 (d, J = 1.9 Hz, 4H, thione), 7.71−7.80 (6H). Anal. Calcd for $C_{56}H_{66}F_{12}Ir_2N_8O_{12}S_8$: C, 35.18; H, 3.48; N, 5.86. Found: C, 35.15; H, 3.22; N, 5.63. MS (ESI, positive ions): m/z 807.1294 (calcd for [M − 2OTf]$^{2+}$ 807.1296).

[Cp$_2$Ir$_2$(μ-**L4**)$_2$](OTf)$_4$ (**4**(OTf)$_4$).* This reaction was carried out as for **1a**(OTf)$_4$, using AgOTf (51 mg, 0.2 mmol), [Cp*$IrCl_2$]$_2$ (40 mg, 0.05 mmol), and **L4** (40 mg, 0.1 mmol) in MeOH solution. **4**(OTf)$_4$ was isolated as a dark green solid (92 mg, 90%). ^{1}H NMR (400 MHz, CD_3OD, ppm): δ 1.73 (s, 30H, Cp*), 3.89 (s, 12H, N-CH_3), 5.34 (s, 8H, −CH_2−), 7.23 (d, J = 6.8 Hz, 8H, Ar-H), 7.39 (s, 4H, thione), 7.46 (d, J = 6.8 Hz, 8H, Ar-H), 7.67 (s, 4H, thione). ^{13}C{^{1}H} NMR (101 MHz, CD_3OD, ppm): δ 10.02 (Cp*-CH_3), 37.12 (N-CH_3), 53.55 (−CH_2−), 96.85 (Cp*-C), 123.64, 125.91, 128.72, 130.63, 134.56, 141.68, 149.64 (C═S). Anal. Calcd for $C_{68}H_{74}F_{12}Ir_2N_8O_{12}S_8$: C, 39.56; H, 3.61; N, 5.43. Found: C, 39.36; H, 3.41; N, 5.49.

[Cp$_2$Ir$_2$(μ-**L5**)$_2$](OTf)$_4$ (**5**(OTf)$_4$).* This reaction was carried out as for **1a**(OTf)$_4$, using AgOTf (51 mg, 0.2 mmol), [Cp*$IrCl_2$]$_2$ (40 mg, 0.05 mmol), and **L5** (27 mg, 0.1 mmol) in MeOH solution. **5**(OTf)$_4$ was isolated as a dark green solid (78 mg, 87%). ^{1}H NMR (400 MHz, CD_3OD, ppm): δ 1.83 (s, 30H, Cp*), 2.57 (m, 4H, −CH_2−), 3.61 (s, 12H, N-CH_3), 4.26 (m, 8H, −CH_2−), 7.33 (4H, thione), 7.50 (4H, thione). Anal. Calcd for $C_{46}H_{62}F_{12}Ir_2N_8O_{12}S_8$: C, 30.90; H, 3.50; N, 6.27. Found: C, 30.49; H, 3.25; N, 6.31.

[Cp$_2$Ir$_2$(μ-**L6**)$_2$](OTf)$_4$ (**6**(OTf)$_4$).* This reaction was carried out as for **1a**(OTf)$_4$, using AgOTf (51 mg, 0.2 mmol), [Cp*$IrCl_2$]$_2$ (40 mg, 0.05 mmol), and **L6** (43 mg, 0.1 mmol) in MeOH solution. **6**(OTf)$_4$ was isolated as a dark green solid (92 mg, 87%). ^{1}H NMR (400 MHz, CD_3CN, ppm): δ 1.85 (s, 30H, Cp*), 3.73 (s, 12H, N-CH_3), 6.30 (s, 8H, −CH_2−), 6.60 (d, J = 2.3 Hz, 4H, thione), 7.21 (d, J = 2.3 Hz, 4H, thione), 7.76−7.78 (m, 8H, Ar-H), 8.45−8.48 (m, 8H, Ar-H). Anal. Calcd for $C_{72}H_{74}F_{12}Ir_2N_8O_{12}S_8$: C, 40.94; H, 3.53; N, 5.30. Found: C, 40.84; H, 3.26; N, 5.47.

[Cp$_2$Ir$_2$(μ-**L7**)$_2$](OTf)$_4$ (**7**(OTf)$_4$).* This reaction was carried out as for **1a**(OTf)$_4$, using AgOTf (51 mg, 0.2 mmol), [Cp*$IrCl_2$]$_2$ (40.0 mg, 0.05 mmol), and **L7** (30 mg, 0.1 mmol) in MeOH solution. **7**(OTf)$_4$ was isolated as a dark green solid (74 mg, 81%). ^{1}H NMR (400 MHz, CD_3OD, ppm): δ 1.55 (s, 30H, Cp*), 4.32 (s, 12H, N-CH_3), 7.93−8.04 (m, 16H, Ar-H and thione). ^{13}C{^{1}H} NMR (101 MHz, CD_3OD, ppm): δ 10.01 (Cp*-CH_3), 46.87 (N-CH_3), 97.01 (Cp*-C), 125.20, 125.85, 128.25, 138.45, 148.67 (C═S). Anal. Calcd for $C_{52}H_{58}F_{12}Ir_2N_8O_{12}S_8$: C, 33.65; H, 3.15; N, 6.04. Found: C, 33.39; H, 3.01; N, 6.32.

General Procedure for H_2-Initiated Transformation Reactions. An NMR tube with J. Young valve was charged with the corresponding 16-electron metallacycle (**1a**(OTf)$_4$ (28.7 mg, 0.015 mmol), **1a**(NO_3)$_4$ (23.4 mg, 0.015 mmol), **2**(OTf)$_4$ (20.0 mg, 0.01 mmol), **3**(OTf)$_4$ (19 mg, 0.01 mmol), or **4**(OTf)$_4$ (20.0 mg, 0.01 mmol)) and CD_3OD (0.6 mL). After freeze−pump−thaw processes, 1 atm of H_2 was charged into the tube at room temperature. A color change from dark green to red was observed in 10 min. After 2 h, the ^{1}H NMR spectrum revealed complete disappearance of the starting material. The crude red crystals were isolated by diffusing diethyl ether into this solution at room temperature for 24 h. They were washed twice with a minimum amount of CH_2Cl_2 and dried under vacuum, yielding pure M_2L_3-type product.

[Cp$_2$Ir$_2$(μ-**L1**)$_3$](OTf)$_4$ (**8**(OTf)$_4$).* This compound was isolated as red crystals (19.6 mg, 0.0089 mmol, 89%). ^{1}H NMR (400 MHz, CD_3OD, ppm): δ 1.51 (s, 30H, Cp*), 3.93 (s, 18H, CH_3), 5.81 (br, 12H, −CH_2−), 7.29−7.45 (m, 24H, Ar-H and thione). ^{13}C NMR (101 MHz, CD_3OD, ppm): δ 8.83 (Cp*-CH_3), 37.66 (N-CH_3), 53.80 (CH_2), 92.63 (Cp*-C), 121.82 (SO_3CF_3, J_{CF} = 321.1 Hz), 122.32 (br, thione), 124.51 (br, thione), 130.27 (Ar-CH), 136.37 (Ar-C), 150. 31 (C═S). ^{19}F NMR (376 MHz, CD_3OD, ppm): δ −79.92. Anal. Calcd for $C_{72}H_{84}F_{12}Ir_2N_{12}O_{12}S_{10}$: C, 38.56; H, 3.78; N, 7.49, Found: C, 38.42; H, 3.97; N, 7.05. MS (ESI, positive ions): m/z 972.2184 (calcd for [M − 2OTf]$^{2+}$ 972.2186).

[Cp$_2$Ir$_2$(μ-**L1**)$_3$](NO$_3$)$_4$ (**8**(NO$_3$)$_4$).* This compound was isolated as red crystals (17.4 mg, 0.0092 mmol, 92%). ^{1}H NMR (400 MHz, CD_3OD, ppm): δ 1.51 (s, 30H, Cp*), 3.94 (s, 12H, N-CH_3), 5.83 (br, 12H, −CH_2−), 7.21−7.32 (m, 18H, Ar-H and thione), 7.47 (d, J = 2.0 Hz, 6H, thione). ^{13}C{^{1}H} NMR (101 MHz, CD_3OD, ppm): δ 8.74 (Cp*-CH_3), 37.59 (N-CH_3), 53.67 (CH_2), 92.62 (Cp*-C), 122.35, 124.50, 130.39 (br), 136.39, 150.31 (C═S). Anal. Calcd for $C_{68}H_{84}Ir_2N_{16}O_{12}S_6$: C, 43.11; H, 4.47; N, 11.83. Found: C, 43.02; H, 4.78; N, 11.52.

[Cp$_2$Ir$_2$(μ-**L2**)$_3$](OTf)$_4$ (**10**(OTf)$_4$).* This compound was isolated as red crystals (14.5 mg, 0.0061 mmol, 92%). ^{1}H NMR (400 MHz, CD_3OD, ppm): δ 1.63 (s, Cp*), 1.66 (CH_3), 1.79 (CH_3), 2.21 (CH_3), 2.30 (CH_3), 2.40 (CH_3), 2.62 (CH_3), 3.83 (N-CH_3), 3.97 (N-CH_3), 4.13 (N-CH_3), 4.81 (d, J = 14.91 Hz, −CH_2−), 4.97 (d, J = 14.91 Hz, −CH_2−), 5.35 (d, J = 14.91 Hz, −CH_2−), 5.51 (d, J = 14.91 Hz, −CH_2−), 6.32 (d, J = 14.91 Hz, −CH_2−), 6.64 (d, J = 14.91 Hz, −CH_2−), 6.88−7.48 (thione and Ar-H). ^{13}C{^{1}H} NMR (101 MHz, CD_3OD, ppm): δ 7.86 (CH_3, Cp*-CH_3), 15.93 (CH_3), 16.67 (CH_3), 17.96 (CH_3), 18.21 (CH_3), 19.13 (CH_3), 19.34 (CH_3), 35.97 (N-CH_3), 36.22 (CH_3), 36.31 (CH_3), 47.11 (CH_2), 48.95 (CH_2), 51.03 (CH_2), 91.02 (Cp*-C), 119.08, 119.28, 120.37, 122.54 (SO_3CF_3, J_{CF} = 320.1 Hz), 122.43, 123.82, 124.08, 127.64, 128.29, 128.51, 130.98, 131.20, 131.29, 139.44, 139.54, 140.39, 147.23 (C═S), 148.46 (C═S), 148.84 (C═S). ^{19}F NMR (376 MHz, CD_3OD, ppm): δ −79.89, −79.91. Anal. Calcd for $C_{81}H_{102}F_{12}Ir_2N_{12}O_{12}S_{10}$: C, 41.07; H, 4.34; N,

7.10. Found: C, 41.32; H, 4.56; N, 7.01. MS (ESI, positive ions): m/z 1035.2490 (calcd for $[M - 2OTf]^{2+}$ 1035.2488).

[Cp$_2$Ir$_2$(μ-L3)$_3$](OTf)$_4$ (11(OTf)$_4$).* This compound was isolated as red crystals (13.5 mg, 0.006 mmol, 90%). ^{1}H NMR (400 MHz, CD_3OD, ppm): δ 1.46 (s, 30H, Cp*), 3.79 (s, 18H, N-CH_3), 5.69 (br, 8H, $-CH_2-$), 7.16 (br, 12H), 7.48 (br, 6H), 7.51 (br, 6H). Anal. Calcd for $C_{72}H_{84}F_{12}Ir_2N_{12}O_{12}S_{10}$: C, 38.56; H, 3.78; N, 7.49. Found: C, 38.39; H, 3.65; N, 7.22.

[Cp$_2$Ir$_2$(μ-L4)$_3$](OTf)$_4$ (12(OTf)$_4$).* This compound was isolated as red crystals (14.3 mg, 0.0058 mmol, 87%). ^{1}H NMR (400 MHz, CD_3OD, ppm): δ 1.55 (s, 30H, Cp*), 3.99 (s, 18H, N-CH_3), 5.90 (s, 12H, $-CH_2-$), 7.28 (s, 24H, Ar-H), 7.37 (s, 6H, thione), 7.52 (d, d, J = 2.0 Hz, 6H, thione). ^{13}C{^{1}H} NMR (101 MHz, CD_3OD, ppm): δ = 9.00 (Cp*-CH_3), 37.92 (N-CH_3), 53.94 ($-CH_2$-), 92.88 (Cp*-C), 122.71, 124.80, 128.45, 130.65, 135.68, 141.70, 150.82 (C═S). Anal. Calcd for $C_{90}H_{96}F_{12}Ir_2N_{12}O_{12}S_{10}$: C, 43.75; H, 3.92; N, 6.80. Found: C, 43.62; H, 3.64; N, 7.10.

Regeneration of 1a(OTf)$_4$. The red solution obtained from the reaction of **1a**(OTf)$_4$ and H_2 in CD_3OD (after 2 h at room temperature, the ^{1}H NMR spectrum showed the signals of **1a**(OTf)$_4$ had disappeared) was heated at 80 °C for 5 h under an argon atmosphere. The solution turned dark green. The ^{1}H NMR spectrum revealed the regeneration of **1a**(OTf)$_4$ with 75% conversion. Crystallization from diethyl ether and MeOH gave **1a**(OTf)$_4$ in 67% yield as dark green crystals.

Regeneration of 2(OTf)$_4$. The red solution obtained from the reaction of **2**(OTf)$_4$ and H_2 in CD_3OD (after 2 h at room temperature, the ^{1}H NMR spectrum showed the signals of **2**(OTf)$_4$ had disappeared) was heated at 80 °C for 5 h under an argon atmosphere. The solution turned dark green. Crystallization from diethyl ether and MeOH gave **2**(OTf)$_4$ in 68% yield as dark green crystals.

[Cp*$_2$Ir$_2$(μ-L2)$_2$](OTf)$_4$ (2(MeCN)$_2$(OTf)$_4$). Dissolution of **2**(OTf)$_4$ in MeCN led instantly to a light yellow solution. ^{1}H NMR (400 MHz, CD_3CN, ppm): δ 1.73−1.78 (30H, Cp*), 2.09−2.11 (6H, CH_3), 2.23−2.31 (12H, CH_3), 3.66−3.70 (12H, N-CH_3), 5.18−5.24 (8H, $-CH_2-$), 6.38−7.33 (10H, thione and Ar-H). ^{13}C{^{1}H} NMR (101 MHz, CD_3CN, ppm): δ 9.28 (Cp*-CH_3), 17.01 (CH_3), 20.73 (CH_3), 37.32 (CH_3), 48.83 (CH_2), 50.06 (N-CH_3), 94.35 (Cp*-C), 120.55, 121.36, 122.15 (SO_3CF_3, J_{CF} = 321.3 Hz), 124.82, 130.65, 132.81, 141.12, 149.46 (C═S). *Note: after removal of the solution under vacuum, a dark green solid was obtained.*

[(Cp*Ir)$_2$(μ-L1)$_2$(CO)$_2$](OTf)$_4$ (1a(CO)$_2$(OTf)$_4$). A solution of 19 mg (0.01 mmol) of **1a**(OTf)$_4$ in 0.6 mL of CD_3OD was shaken under 1 atm of CO. A rapid color change from dark green to yellow was observed. The conversion was quantitative. ^{1}H NMR (400 MHz, CD_3OD, ppm): δ 2.00 (s, 15H, Cp*), 2.01 (s, 15H, Cp*), 3.84 (s, 6H, N-CH_3), 3.87 (s, 6H, N-CH_3), 5.45−5.64 (m, 8H, $-CH_2-$), 7.27 (s, 4H, Ar-H), 7.34 (s, 4H, Ar-H), 7.50 (d, J = 2.01 Hz, 2H, thione), 7.58 (d, J = 2.01 Hz, 2H, thione), 7.66 (m, 4H, thione). ^{13}C{^{1}H} NMR (101 MHz, CD_3OD, ppm): δ 9.15 (Cp*-CH_3), 9.16 (Cp*-CH_3), 37.80 (N-CH_3), 37.81 (N-CH_3), 53.83 (CH_2), 53.87 (CH_2), 106.02 (Cp*-C), 106.07 (Cp*-C), 123.90, 123.98, 124.76 (SO_3CF_3, J_{CF} = 321.1 Hz), 125.71, 125.77, 129.82, 129.90, 136.17, 136.37, 147.06 (C═S), 147.13 (C═S), 170.04 (C═O), 170.16 (C═O).

[(Cp*Ir)$_2$(μ-L2)$_2$(Py)$_2$](OTf)$_4$ (2(Py)$_2$(OTf)$_4$). Pyridine (4 mg, 0.05 mmol) was added to a solution of **2**(OTf)$_4$ (50 mg, 0.025 mmol) in CH_3OH (20 mL) at room temperature, and the mixture was stirred for 3 h. A color change from dark green to yellow was observed. The solvent was concentrated to about 3 mL. Diethyl ether was added slowly to the solution, and the product was isolated by filtration. The resulting yellow solid was dried under vacuum to give **2**(Py)$_2$(OTf)$_4$ (47 mg, 87%). ^{1}H NMR (400 MHz, [D$_6$]-DMSO, ppm): δ 1.57 (s, 30H, Cp*), 2.13 (s, 6H, CH_3), 2.39 (s, 12H, CH_3), 3.66 (12H, N-CH_3), 5.32 (8H, $-CH_2-$), 7.10−8.58 (20H, Ar-H, thione and pyridine). Anal. Calcd for $C_{72}H_{88}F_{12}Ir_2N_{10}O_{12}S_8$: C, 40.14; H, 4.12; N, 6.50. Found: C, 40.31; H, 4.37; N, 6.18.

[(Cp*Ir)$_2$(μ-L2)$_2$Cl$_2$](OTf)$_2$ (2(Cl)$_2$(OTf)$_2$). NaCl (2 mg, excess) was added to a solution of **2**(OTf)$_4$ (20 mg, 0.01 mmol) in CH_3OH (5 mL) at room temperature, and the mixture was stirred for 3 h, followed by filtration to remove insoluble compounds. A color change from dark green to red was observed. The solvent was concentrated to about 1 mL. Diethyl ether was added slowly to the solution, and the product was isolated by filtration. The resulting orange-red solid was dried under vacuum to give **2**(Cl)$_2$(OTf)$_2$ (15 mg, 85%). ^{1}H NMR (400 MHz, [D$_6$]-DMSO, ppm): δ 1.71 (s, 30H, Cp*), 2.05 (s, 6H, CH_3), 2.22 (s, 12H, CH_3), 3.50, 3.70 (12H, N-CH_3), 5.06, 5.16 (8H, $-CH_2-$), 6.32−6.37 (m, 2H, thione), 6.78−6.82 (m, 2H, thione), 6.32−6.38 (m, 2H, thione), 6.32−6.37 (m, 2H, thione), 7.08−7.12 (m, 4H, thione and Ar-H), 7.56 (m, 2H, thione). Anal. Calcd for $C_{60}H_{78}Cl_2F_6Ir_2N_8O_6S_6$: C, 40.74; H, 4.44; N, 6.33. Found: C, 40.49; H, 4.63; N, 6.42. MS (ESI, positive ions): m/z 1619.3379 (calcd for $[M - OTf]^+$ 1619.3380).

Synthesis of 2(OTf)$_4$ from 2(Cl)$_2$(OTf)$_2$. AgOTf (26 mg, 0.1 mmol) was added to a solution of **2**(Cl)$_2$(OTf)$_2$ (88 mg, 0.05 mmol) in CH_3OH (20 mL) at room temperature, and the mixture was stirred for 3 h. A color change from red to dark blue was observed. After filtration, the solvent was concentrated to about 3 mL. Diethyl ether was added slowly to the solution, and the product was isolated by filtration. Yield: 88 mg, 88%.

X-ray Crystallography Details. Diffraction data were collected on a Bruker AXS APEX CCD diffractometer equipped with a rotating anode using graphite-monochromated Mo Kα radiation (λ = 0.71073 Å).[39] Diffraction data were collected over the full sphere and were corrected for absorption. The structures were solved by direct methods using SHELXS and refined against F^2 on all data by full-matrix least squares with SHELXL-97.[40,41] Additional details can be found in the Supporting Information.

■ ASSOCIATED CONTENT

Supporting Information

Text, figures, tables, and CIF files giving synthesis and characterization details of thione ligands **L1**−**L7**, structures of **9**(OTf) and **L2**, bond distances and angles and crystal data and structure refinement details for all compounds, and X-ray crystallographic data for **L2**, **1a**(OTf)$_4$, **1a**(NO$_3$)$_4$, **1a**(BF$_4$)$_4$, **1b**(OTf)$_4$, **3**(OTf)$_4$, **5**(OTf)$_4$, **6**(OTf)$_4$, **7**(OTf)$_4$, **8**(OTf)$_4$, **8**(NO$_3$)$_4$, **9**(OTf), **10**(OTf)$_4$, **12**(OTf)$_4$, [**2**(Py)$_2$](OTf)$_4$, and [**2**(Cl)$_2$](OTf)$_2$. This material is available free of charge via the Internet at http://pubs.acs.org.

■ AUTHOR INFORMATION

Corresponding Authors

*E-mail for Y.-F.H.: yfhan1980@fudan.edu.cn.

*E-mail for G.-X.J.: gxjin@fudan.edu.cn.

Notes

The authors declare no competing financial interest.

■ ACKNOWLEDGMENTS

This work was supported by the NSFC (21371036, 91122017, 21001029), PCSIRT (IRT1117), Shanghai Pujiang Program (14PJD006), Shanghai Rising-Star Program (11QA1400300), and Shanghai Science and Technology Committee (13JC1400600, 13DZ2275200).

■ REFERENCES

(1) Ertl, G.; Knöinger, H.; Schüth, F.; Weitkamp, J. *Handbook of Heterogeneous Catalysis*; Wiley-VCH: Weinheim, Germany, 2008.

(2) Hartwig, J. *Organotransition Metal Chemistry*; University Science Books: Sausalito, CA, 2010.

(3) (a) Evans, D. J.; Pickett, C. J. *Chem. Soc. Rev.* **2003**, *32*, 268−275. (b) Ogo, S. *Chem. Commun.* **2009**, 3317−3325.

(4) (a) Fonecilla-Camps, J. C.; Volbeda, A.; Cavazza, C.; Nicolet, Y. *Chem. Rev.* **2007**, *107*, 4273−4303. (b) Lubitz, W.; Ogata, H.; Rüdiger, O.; Reijerse, E. *Chem. Rev.* **2014**, *114*, 4081−4148.

(5) (a) Welch, G. C.; San Juan, R. R.; Masuda, J. D.; Stephan, D. W. *Science* **2006**, *314*, 1124−1126. (b) Stephan, D. W.; Erker, G. *Angew. Chem., Int. Ed.* **2010**, *49*, 46−76.
(6) Spikes, G. H.; Fettinger, J. C.; Power, P. P. *J. Am. Chem. Soc.* **2005**, *127*, 12232−12233.
(7) (a) Chapman, A. M.; Haddow, M. F.; Wass, D. F. *J. Am. Chem. Soc.* **2011**, *133*, 18463−18478. (b) Chapman, A. M.; Haddow, M. F.; Wass, D. F. *J. Am. Chem. Soc.* **2011**, *133*, 8826−8829.
(8) Kuwata, S.; Ikariya, T. *Dalton Trans.* **2010**, *39*, 2984−2992.
(9) Heinekey, D. M.; Lledos, A.; Lluch, J. M. *Chem. Soc. Rev.* **2004**, *33*, 175−182.
(10) Rakowski Dubois, M.; Dubois, D. L. *Acc. Chem. Res.* **2009**, *42*, 1974−1982.
(11) (a) McGrady, G.; Guilera, S. G. *Chem. Soc. Rev.* **2003**, *32*, 383−392. (b) Gloaguen, F.; Rauchfuss, T. B. *Chem. Soc. Rev.* **2009**, *38*, 100−108.
(12) Kubas, G. J. *Chem. Rev.* **2007**, *107*, 4152−4205.
(13) (a) Harman, W. H.; Peters, J. C. *J. Am. Chem. Soc.* **2012**, *134*, 5080−5082. (b) Harman, W. H.; Lin, T.-P.; Peters, J. C. *Angew. Chem., Int. Ed.* **2014**, *53*, 1081−1086.
(14) Van Leeuwen, P. W. N. M. *Homogeneous Catalysis. Understanding the Art*; Kluwer Academic: Dordrecht, The Netherlands, 2004.
(15) (a) Poli, R. *Chem. Rev.* **1996**, *96*, 2135−2204. (b) Nagashima, H.; Kondo, H.; Hayashida, T.; Yamaguchi, Y.; Gondo, M.; Masuda, S.; Miyazaki, K.; Matsubara, K.; Kirchner, K. *Coord. Chem. Rev.* **2003**, *245*, 177−190. (c) Clapham, S. E.; Hadzovic, A.; Morris, R. H. *Coord. Chem. Rev.* **2004**, *248*, 2201−2237. (d) Noyori, R.; Sandoval, C. A.; Muniz, K.; Ohkuma, T. *Philos. Trans. R. Soc. London* **2005**, *363*, 901−912. (e) Ikariya, T.; Murata, K.; Noyori, R. *Org. Biomol. Chem.* **2006**, *4*, 393−406.
(16) Liu, S.; Han, Y.-F.; Jin, G.-X. *Chem. Soc. Rev.* **2007**, *36*, 1543−1560.
(17) Ohki, Y.; Sakamoto, M.; Tatsumi, K. *J. Am. Chem. Soc.* **2008**, *130*, 11610−11611.
(18) Suzuki, T. *Chem. Rev.* **2011**, *111*, 1825−1845.
(19) Valpuesta, J. E.; Rendón, N.; López-Serrano, J.; Poveda, M. L.; Sánchez, L.; Álvarez, E.; Carmona, E. *Angew. Chem., Int. Ed.* **2012**, *51*, 7555−7557.
(20) (a) White, C.; Oliver, A. J.; Maitlis, P. M. *J. Chem. Soc., Dalton Trans.* **1973**, 1901−1907. (b) Maitlis, P. M. *Acc. Chem. Res.* **1978**, *11*, 301−307. (c) Gilbert, T. M.; Bergman, R. G. *J. Am. Chem. Soc.* **1985**, *107*, 3502−3507.
(21) Rauchfuss, T. B. *J. Am. Chem. Soc.* **2006**, *128*, 13048−13049.
(22) (a) Leininger, S.; Olenyuk, B.; Stang, P. J. *Chem. Rev.* **2000**, *100*, 853−908. (b) Northrop, B. H.; Zheng, Y.-R.; Chi, K.-W.; Stang, P. J. *Acc. Chem. Res.* **2009**, *42*, 1554−1563. (c) Chakrabarty, R.; Mukherjee, P. S.; Stang, P. J. *Chem. Rev.* **2011**, *111*, 6810−6918. (d) Han, M.; Engelhard, D. M.; Clever, G. H. *Chem. Soc. Rev.* **2014**, *43*, 1848−1860. (e) Castilla, A. M.; Ramsy, W. J.; Nitschke, J. R. *Acc. Chem. Res.* **2014**, *47*, 2063−2073.
(23) (a) Balzani, V.; Credi, A.; Raymo, F. M.; Stoddart, J. F. *Angew. Chem., Int. Ed.* **2000**, *39*, 3348−3391. (b) Lehn, J.-M. *Chem. Soc. Rev.* **2007**, *36*, 151−160.
(24) Ramstrom, O.; Lehn, J.-M. *Nat. Rev. Drug Discovery* **2002**, *1*, 26−36.
(25) Steed, J. W.; Atwood, J. L. *Supramolecular Chemistry*, 2nd ed.; Wiley: Hoboken, NJ, 2009.
(26) (a) Sun, S.-S.; Anspach, J. A.; Lees, A. J. *Inorg. Chem.* **2002**, *41*, 1862−1869. (b) Saalfrank, R. W.; Demleitner, B.; Glaser, H.; Maid, H.; Bathelt, D.; Hampel, F.; Bauer, W.; Teichert, M. *Chem. Eur. J.* **2002**, *8*, 2679−2683. (c) Sun, S.-S.; Stern, C. L.; Nguyen, S. T.; Hupp, J. T. *J. Am. Chem. Soc.* **2004**, *126*, 6314−6326. (d) Clever, G. H.; Tashiro, S.; Shionoya, M. *J. Am. Chem. Soc.* **2010**, *132*, 9973−9975. (e) Wang, J. B.; Kulago, A.; Browne, W. R.; Feringa, B. L. *J. Am. Chem. Soc.* **2010**, *132*, 4191−4196. (f) Chen, S.; Chen, L.-J.; Yang, H.-B.; Tian, H.; Zhu, W. *J. Am. Chem. Soc.* **2012**, *134*, 13596−13599. (g) Han, M.; Michel, R.; He, B.; Chen, Y.-S.; Stalke, D.; John, M.; Clever, G. H. *Angew. Chem., Int. Ed.* **2013**, *52*, 1319−1323. (h) Chen, L.-J.; Zhao, G.-Z.; Jiang, B.; Sun, B.; Wang, M.; Xu, L.; He, J.; Abliz, Z.; Tan, H.; Li, X.; Yang, H.-B. *J. Am. Chem. Soc.* **2014**, *136*, 5993−6001. (i) Li, Z.-Y.; Zhang, Y.; Zhang, C.-W.; Chen, L.-J.; Wang, C.; Tan, H.; Yu, Y.; Li, X.; Yang, H.-B. *J. Am. Chem. Soc.* **2014**, *136*, 8577−8589. (j) Zhao, L.; Northrop, B. H.; Stang, P. J. *J. Am. Chem. Soc.* **2008**, *130*, 11886−11888.
(27) Zheng, Y.-R.; Zhao, Z.; Wang, M.; Ghosh, K.; Pollock, J. B.; Cook, T. R.; Stang, P. J. *J. Am. Chem. Soc.* **2010**, *132*, 16873−16882.
(28) Neogi, S.; Lorenz, Y.; Engeser, M.; Samanta, D.; Schmittel, M. *Inorg. Chem.* **2013**, *52*, 6975−6984.
(29) For reviews, see: (a) Gianneschi, N. C.; Masar, M. S., III; Mirkin, C. A. *Acc. Chem. Res.* **2005**, *38*, 825−837. (b) Oliveri, C. G.; Ulmann, P. A.; Wiester, M. J.; Mirkin, C. A. *Acc. Chem. Res.* **2008**, *41*, 1618−1629. For one recent example, see: Mendez-Arroyo, J.; Barroso-Flores, J.; Lifschitz, A. M.; Sarjeant, A. A.; Stern, C. L.; Mirkin, C. A. *J. Am. Chem. Soc.* **2014**, *136*, 10340−10348.
(30) (a) Gianneschi, N. C.; Bertin, P. A.; Nguyen, S. T.; Mirkin, C. A.; Zakharov, L. N.; Rheingold, A. L. *J. Am. Chem. Soc.* **2003**, *125*, 10508−10509. (b) Gianneschi, N. C.; Cho, S.-H.; Nguyen, S. T.; Mirkin, C. A. *Angew. Chem., Int. Ed.* **2004**, *43*, 5503−5507. (c) Kuwabara, J.; Stern, C. L.; Mirkin, C. A. *J. Am. Chem. Soc.* **2007**, *129*, 10074−10075. (d) Masar, M. S., III; Gianneschi, N. C.; Oliveri, C. G.; Stern, C. L.; Nguyen, S. T.; Mirkin, C. A. *J. Am. Chem. Soc.* **2007**, *129*, 10149−10158.
(31) Lavallo, V.; El-Batta, A.; Bertrand, G.; Grubbs, R. H. *Angew. Chem., Int. Ed.* **2011**, *50*, 268−271.
(32) Lavallo, V.; Grubbs, R. H. *Science* **2009**, *326*, 559−562.
(33) During this process, the formation of protonated compounds should be involved, as evidenced by the reaction solution becoming acidic. In addition, a long reaction afforded some unidentified metal hydride species. For the relation of hydride species, see: (a) Hou, Z.; Koizumi, T.; Fujita, A.; Yamazaki, H.; Wakatsuki, Y. *J. Am. Chem. Soc.* **2001**, *123*, 5812−5813. (b) Kristjánsdóttir, S. S.; Norton, J. R. Acidity of Hydrido Transition Metal Complexes in Solution. In *Transition Metal Hydrides*; Dedieu, A., Ed.; VCH: New York, 1991; pp 309−359. (c) Jessop, P. G.; Morris, R. H. *Coord. Chem. Rev.* **1992**, *121*, 155−284.
(34) For the structural characterization of $[Cp^*_2Ir_2(\mu\text{-}H)_3](X)$ (X = BF_4, ClO_4), see also: (a) Bau, R.; Teller, R. G.; Kirtley, S. W.; Koetzle, T. F. *Acc. Chem. Res.* **1979**, *12*, 176−183. (b) Stevens, R. C.; Mclean, M. R.; Wen, T.; Carpenter, J. D.; Bau, R.; Koetzle, T. F. *Inorg. Chim. Acta* **1989**, *161*, 223−231.
(35) Stephenson, A.; Argent, S. P.; Riis-Johannessen, T.; Tidmarsh, I. S.; Ward, M. D. *J. Am. Chem. Soc.* **2011**, *133*, 858−870.
(36) (a) Hahn, F. E.; Seidel, W. W. *Angew. Chem., Int. Ed. Engl.* **1995**, *34*, 2700−2703. (b) Su, C.-Y.; Cai, Y.-P.; Chen, C.-L.; Smith, M. D.; Kaim, W.; zur Loye, H.-C. *J. Am. Chem. Soc.* **2003**, *125*, 8595−8613. (c) Hahn, F. E.; Offermann, M.; Pape, T.; Frölich, R. *Angew. Chem. Int. Ed.* **2008**, *47*, 6794−6797.
(37) White, C.; Yates, A.; Maitlis, P. M. *Inorg. Synth.* **1992**, *29*, 228.
(38) (a) Jia, W.-G.; Huang, Y.-B.; Lin, Y.-J.; Jin, G.-X. *Dalton Trans.* **2008**, 5612−5620. (b) Roy, G.; Jayaram, P. N.; Mugesh, G. *Chem. Asian J.* **2013**, *8*, 1910−1921.
(39) *SMART*; Bruker AXS, Madison, WI, USA, 2000.
(40) *SHELXS*-97: Sheldrick, G. M. *Acta Crystallogr., Sect. A* **1990**, *A46*, 467−473.
(41) *SHELXS*-97: Sheldrick, G. M. *Acta Crystallogr., Sect. A* **2008**, *A64*, 112−122.